Nuclear astrophysics in storage rings

C.A. Bertulani *

Instituto de Física, Universidade Federal do Rio de Janeiro 21945-970, Rio de Janeiro, RJ, Brazil

Nuclear reaction cross sections are usually very small in typical astrophysical environments. It has been one of the major challenges of experimental nuclear astrophysics to assess the magnitude of these cross sections in the laboratory. For a successful experiment high luminosity beams are needed. Increasing the target width, one also increases the reaction yields. But, this is of limited use due to multiple scattering in the target. Storage rings are appropriate tools to overcome these difficulties. Storage rings can work with large luminosities, and the beams cross the interaction region many times per second (typically one million/s), compensating low density internal gas targets, or low reaction rates in beam-beam collisions. Storage rings are also ideal tools for precise measurements of masses and beta-decay lifetimes of nuclei of relevance for astrophysics.

1. CENTRAL PROBLEMS IN NUCLEAR ASTROPHYSICS

1.1. Screening

Nuclear astrophysics requires the knowledge of the reaction rate R_{ij} between the nuclei i and j. It is given by $R_{ij} = n_i n_j < \sigma v > /(1 + \delta_{ij})$, where σ is the cross section, v is the relative velocity between the reaction partners, n_i is the number density of the nuclide i, and $<>$ stands for energy average. Extrapolation procedures are often needed to obtain cross sections in the energy region of astrophysical relevance. While non-resonant cross sections can be rather well extrapolated to the low-energy region, the presence of continuum, or subthreshold resonances, complicates these extrapolations. Another problem is that charged-particle induced reactions are electron-screened in stellar environments [1]. Applying the Debye-Hückel approach, one finds that the plasma enhances reaction rates, e.g., $^3He(^3He, 2p)^4He$ and $^7Be(p, \gamma)^8B$, by as much as 20%. Laboratory nuclear reactions are also modified by screening effects due to electrons which are inevitably present in the target [2]. As can be seen in figure 1 for the reaction $^3He(d, p)^4He$ (probably the best studied example of laboratory electron screening effects, both experimentally and theoretically - Data are from ref. [3]. Calculations are from ref. [4]), the effects of laboratory electron screening are far from being understood and require further investigation.

While corrections due to plasma screening effects have to rely on theoretical models, laboratory screening can be avoided experimentally using crossed beams in storage rings.

This might be of great usefulness for the study of the reactions $^6Li(d, \alpha)^4He$,$^7Li(p, \alpha)^4He$,-$^{11}B(p, \alpha)2$ ^4He, and $^6Li(p, \alpha)^3He$, where discrepancies between experiment and theoretical calculations of electron screening are large [5].
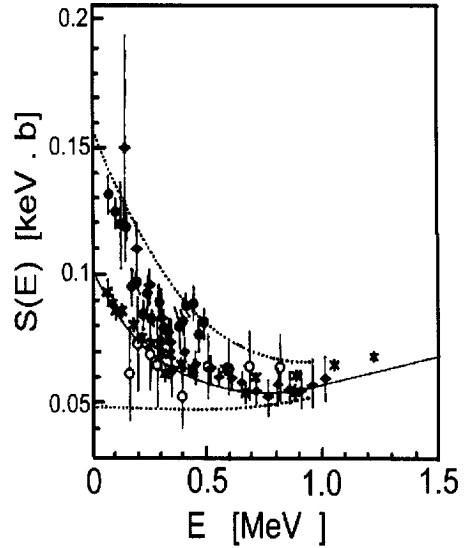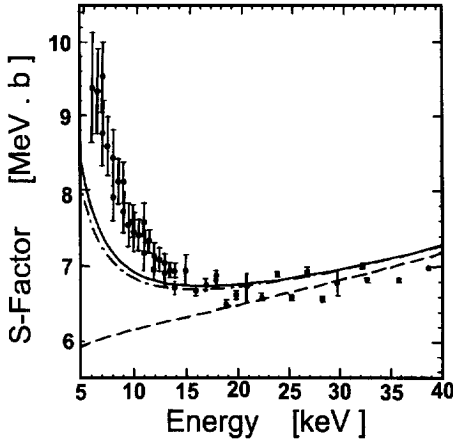

Figure 1.   The $^3He(d, p)^4He$ S-factors. Dashed line is the calculated astrophysical S-factor for bare nuclei. Solid and dot-dashed curves include corrections of screening.

Figure 2.   Astrophysical S-factor for $^4He(^3H, \gamma)^7Li$ compared to a theoretical calculation (solid curve). The data imply that S-factors could be anything in the region limited by the dashed curves.

1.2. Homogeneous Big Bang

Deuterons were formed by fusion of neutrons and protons when the Universe temperature reached $T = 10^{12}$ K. However, they were promptly dissociated by photons which existed in thermal equilibrium. Only when $T \sim 10^9$ K deuterons were formed in significant concentration and the primordial nucleosynthesis bottleneck was overcome. Since, (i) the binding energies of ^3He and ^4He are larger than that of the deuteron and (ii) the cross sections for capture of protons and neutrons by deuterons are large, and deuterons were rapidly consumed. Standard primordial nucleosynthesis assumes a homogeneous proton-to-neutron density. Thus the nuclear reaction flow along the $Z \sim N$ stability line stops at ^8B because of its instability. Since the element with A=5 does not exist, ^4He is by far the most abundant product of primordial nucleosynthesis. Only rather small traces of D, ^3He and ^7Li are made. Just because of that, the relative abundances of these elements are a good test of the Big Bang scenario. Among the several reactions relevant for primordial nucleosynthesis, the radiative capture reaction $^4He(^3H, \gamma)^7Li$ deserves special attention. There has been a large discrepancy among five measured cross sections for this reaction, as shown in figure 2 (adapted from [6]). This leads to an error of order of 30% - 40% in the primordial ^7Li abundance and also in the determination of the cosmological parameter

Ω_B [6].

1.3. Inhomogeneous Big Bang

Inhomogeneous Big Bang models allow for fluctuations in baryon densities that are related to different neutron mass fractions at the beginning of nucleosynthesis. These models involve some nuclear reactions of which cross sections were not known. The postulated dominant flow path, which bypasses the A=8 gap, is $^4He(t, \gamma)^7Li(n, \gamma)$ $^8Li(\alpha, n)^{11}B(n, \gamma)^{12}B(\beta^-\nu)^{12}C$. Here, the $^8Li(\alpha, n)^{11}B$ reaction was completely unknown. The first experiment was made using the reverse reaction $^{11}B(n, \alpha)^8Li$, finding a large resonance at around 0.5 MeV above the α threshold in ^{12}B [7]. This energy corresponds to the Gamow peak of 10^9 K, which is a typical temperature for heavy elemental synthesis in the primordial site. However, this reaction has been measured directly using a low-energy ^8Li beam at $E_{c.m.} \geq 1.5$ MeV [8] at RIKEN. The cross section estimated by an extrapolation to $E_{c.m.} \sim 0.5$ MeV is larger than the previous value [7] by roughly a factor of 5. The reason for the difference between the two results is that the inverse process uses a stable ^{11}B beam. Thus, only the cross section for the transition to the ground state was determined by using the principle of detailed balance. However, there are at least four more excited bound states of ^{11}B which contribute to the production of ^{11}B through $^8Li(\alpha, n)^{11}B^*(\gamma)^{11}B$. This is a very interesting subject to be pursued by a direct measurement at $E_{c.m.} \sim 0.5$ and shows the importance of radioactive beam facilities for astrophysical purposes.

1.4. The Sun

Because of the work of Bahcall and collaborators, there seems to be a very consistent understanding of the hydrodynamics and the nuclear reaction network in the Sun [9]. The main network for energy production in the sun is the well known ppI-chain, with the net result of fusing four protons to form one tightly bound ^4He nucleus. In a 14% branch, a ^7Be nucleus is produced via the $^3He + ^4He \rightarrow ^7Be + \gamma$ radiative capture process. In a very rare event, the ^7Be nucleus will capture a proton to form ^8B, which subsequently decays via positron emission to an excited state of ^8Be; this state, in turn, rapidly breaks into two α-particles. This is the ppIII chain:

$$p(p, e^+\nu)d(p, \gamma)^3He(^4He, \gamma)^7Be(p, \gamma)^8B(e^+\nu)^8Be^* \rightarrow 2\ ^4He . \tag{1}$$
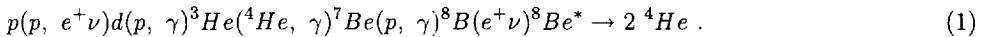
Although this chain delivers a very small part of the energy produced in the sun, it is responsible for the emission of high-energy neutrinos. These high energy neutrinos play an important role in the history of the search for solar neutrinos. Terrestrial detection of solar neutrinos have lead to the conclusion that an appreciable part of these neutrinos are missing. This is known as the *solar neutrino problem*, which persists for about two decades [9]. Due to the Coulomb barrier, the reaction cross section $^7Be(p, \gamma)^8B$ is very small at the Gamow peak (~ 20 keV). Direct measurements have reached $E_{p-Be} \sim 140$ keV. However, discrepancies among experimental data are evident as shown in figure 3. Long ago, Barker [10] has emphasized that an analysis of the existing experimental data yields an S-factor for this reaction at low energies which is uncertain by as much as 30%. This situation has not changed. A measurement of this reaction at the Gamow peak is highly desirable.

1.5. Massive Stars

1.5.1. The $^{12}C(\alpha, \gamma)^{16}O$ reaction

We now consider a massive star, of order of 25 solar masses. After hydrogen burning, when the temperature and the density of the core of the star reaches values of $T \sim 1.5 \times 10^8$ K and $\rho \sim 5 \times 10^4$ g/cm^3, helium can react with helium to form ^{12}C. This happens via an s-wave resonance ($E = 92$ keV) in ^8Be, with mean lifetime close to 10^{-16} s. This lifetime is long enough that a small amount of ^8Be is formed and captures an α-particle to form ^{12}C. The cross section for this reaction is enhanced by the existence of a resonance at 287 keV in ^{12}C above the $\alpha +^8 Be$ threshold. This was predicted by Hoyle before the state was confirmed experimentally [11]. The ^{12}C produced can capture an α-particle to form ^{16}O. This $^{12}C(\alpha, \gamma)^{16}O$ reaction is a key process for the elemental abundances of heavy elements, and for the evolution of the stars. It is argued that the cross section for this reaction should be known to better than 20%, for a good modeling of the stars [12]. This goal has not yet been achieved.

The problem with the experimental determination of the $^{12}C(\alpha, \gamma)^{16}O$ reaction at the energy $E \sim 300$ keV ($T \sim 2 \times 10^8$ K) is the existence of a broad 1^- resonance at $E = 2.42$ MeV above the $\alpha +^{12} C$ threshold, as well as two sub-threshold states: a 1^- state just 45 keV below the threshold, and a 2^+ state 245 keV below threshold. These states interfere and their contribution to the data cannot be separated unambiguously. Theoretical calculations of this reaction are also not reliable, as this process is, in first order isospin forbidden and proceeds via unknown $T = 1$ impurities in the ^{16}O compound nuclear states. Recently, the $E1$ radiative capture contribution to this reaction was obtained by the beta-delayed emission of α-particles from a 2^- state in $^{16}N(t_{1/2} = 7.1$ $s)$ [13]. Due to the beta-decay selection rules, excited states in ^{16}O with $J^\pi = 1^-$, 2^-, and 3^- are populated. Thus, only $E1$ transitions in the alpha decay are possible. It is expected however, that $E2$ transitions in the radiative capture reaction $^{12}C(\alpha, \gamma)^{16}O$ are as well important as $E1$ transitions. The total capture cross section, $\sigma_{E1} + \sigma_{E2}$ is therefore still unknown with the required precision.

1.5.2. Rapid capture processes

With increasing temperatures and densities of the core the star reaches advanced burning stages. Then carbon burning ($T \sim 5 \times 10^8$ K, $\rho = 1 - 2 \times 10^5$ g/cm^3) is followed by neon burning ($T \sim 5 \times 10^8$ K, $\rho = 4 \times 10^6$ g/cm^3), oxygen burning ($T \sim 1.5 \times 10^9$ K, $\rho = 10^7$ g/cm^3) and silicon burning cycles ($T \sim 3 \times 10^9$ K, $\rho = 3 \times 10^7$ g/cm^3). The star then forms ^{56}Fe which is the end point of spontaneous nuclear fusion. The energy released by nuclear fusion stops and the core collapses due to gravitation pressure. The iron nuclei are broken up, absorbing energy from the plasma, and accelerating the collapse. The high density of the core favors electron capture, transforming protons in neutrons and emitting neutrinos, which escape from the star. When the core density reaches densities of about 2.4×10^{14} g/cm^3 (nuclear matter density), it cannot contract further, bounces back, and a shockwave will run through the outer layers of the collapsed star. However, this shockwave does not carry enough energy to explode the star. The shock is heating the material to such high temperatures that the previously produced iron is photo disintegrated again. This process takes 4–7 MeV per nucleon (7 MeV for a complete photo disintegration into nucleons) and will eventually halt the shockfront. The formation of the neutron star

leads to a gain in gravitational binding energy which is released in the form of neutrinos. Although the interaction of neutrinos with matter is quite weak, considerable amounts of energy can reheat the outer layers even if only 1% of the 10^{53} erg (10^{46} J) in neutrinos is deposited via neutrino captures on neutrons and protons. This accelerates the shockwave again and can finally explode the star. Because of the heating and expansion of the gas, a zone with low density and high temperature will be formed behind the shockfront, the so–called *high–entropy bubble*.

During the subsequent cooling of the plasma the nucleons will recombine again, first to α–particles, then to heavier nuclei, starting with the reactions $3\alpha \rightarrow {}^{12}C$ and $\alpha + \alpha + n \rightarrow {}^9Be$, followed by ${}^9Be(\alpha,n){}^{12}C$. Temperature and density are dropping quickly in the adiabatically expanding high–entropy bubble. This will hinder the recombination of alpha particles into heavy nuclei, leaving a high Y_n/Y_{seed} and sufficient neutrons for an r–process, (acting on the newly produced material) at the end of the α–process after freeze–out of charged particle reactions. Approximately half of all stable nuclei observed in nature in the heavy element region about $A > 60$ is produced in the r–process. This r–process occurs in environments with large neutron densities which lead to $\tau_n \ll \tau_\beta$.
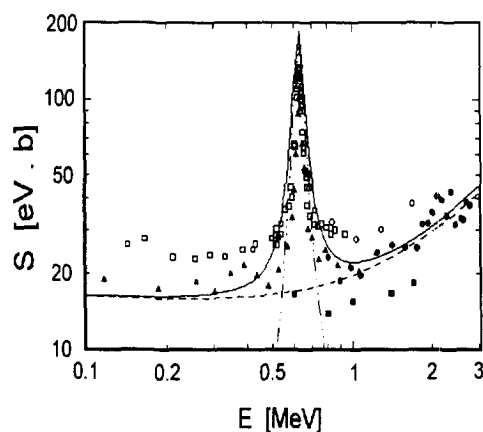

Figure 3. S-factors for ${}^7Be(p, {}^8Be)$ from several experiments. Curves are theoretical calculations based on a potential model.
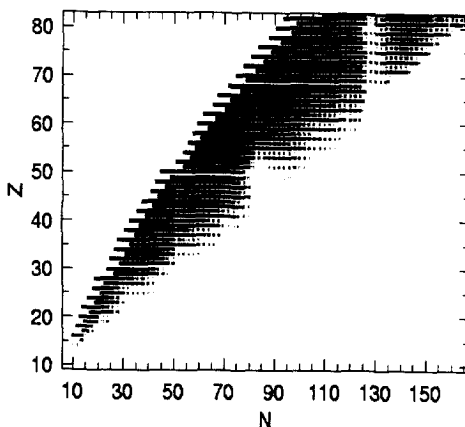
Figure 4. Level density (in levels per MeV) at the respective neutron separation energy. Higher level densities are represented by darker cells.

The most neutron–rich isotopes along the r–process path have lifetimes of less than one second and more typically 10^{-2} to 10^{-1} s. Cross sections for most of the nuclei involved cannot be experimentally measured due to the short half–lives. Therefore, theoretical descriptions of the capture cross sections as well as the beta–decay half–lives are the only source of the nuclear physics input for r–process calculations. For nuclei with about

$Z > 80$ beta–delayed fission and neutron–induced fission might also become important (for a review, see [14]).

2. COSMOCHRONOMETRY

Presently, the most important application of storage rings to nuclear astrophysics has been the determination of *bound-β-decay* lifetimes. An ingenuous experiment performed with the heavy-ion storage ring ESR at GSI/Darmstadt measured the β-decay half-life of bare ^{163}Dy [15]. The $^{163}Dy^{66+}$ ions were stored and accumulated in the ring. Contrary to neutral atoms the electron originating from β-decay of bare nuclei can occupy one of the atomic orbits in the nucleus. This reduces dramatically the β-decay half-lives of several nuclei, or can be the only way that the β-decay can proceed. In fact, the experiment deduced a half-life of 47^{+5}_{-4} d for bare ^{163}Dy, which is stable as a neutral atom.

More recently [16], the same method was used to study the bound β-transitions in bare ^{187}Re. The observed (preliminary) half-life of 34 ± 7 yr is much smaller than the neutral atom half-life, $T_{1/2} = 43\ Gyr$ [$1\ Gyr = 10^9\ yr$]. This result has a great influence on the use of the $^{187}Re - ^{187}Os$ as a cosmochronometer isotopic pair. The *astration* of ^{187}Re in the hot environment of next generation stars may involve bare, or almost bare, ^{187}Re nuclei, and induces a big difference on the derivation of the Galactic age from the $^{187}Os/^{187}Re$ relative abundance [16].

There is a proposal to measure the bound β-decay of bare ^{205}Tl [17]. This nucleus can be transmuted to ^{205}Pb by solar neutrino capture. Thus, a measurement of the $^{205}Tl/^{205}Pb$ abundance ratio in deep lying rocks can give the information on the solar neutrino flux integrated over 10^7 yr. The neutrino capture goes to the first-excited state of ^{205}Pb and the experiment aims in providing this nuclear transition matrix element which is unknown.

The subject of bound β-decay experiments is discussed in more details by O. Keppler in these proceedings.

3. DETERMINATION OF ASTROPHYSICAL NUCLEAR RATES

To calculate astrophysical reaction rates with some reliability, one needs to know several nuclear properties which have to be assessed experimentally. Here we give some examples of what can be studied with storage rings.

3.1. Elastic Scattering and (p, p′) reactions

The use of internal proton gas targets is a standard technique in storage rings. Protons are a very useful probe since their internal structure remains unaffected during low energy collisions. Nuclear densities are a basic input in theoretical calculations of astrophysical reactions at low energies. These can be obtained in, e.g., elastic proton scattering. Elastic scattering in high energy collisions essentially measures the Fourier transform of the matter distribution. Considering for simplicity the one-dimensional case, for light nuclei one has $\int e^{iqx}\rho(x)dx \sim \int e^{iqx}[a^2 + x^2]^{-1} = (\pi/a).e^{-|q|a}$, where $q = 2k\sin\theta/2$, for a c.m. momentum k, and a scattering angle θ. For heavy nuclei the density ρ is better described by Fermi function, and $\int e^{iqx}[1 + e^{(x-R)/a}]^{-1} \sim (4\pi).\sin qR.e^{-\pi qa}$, for $R >> a$, and $qa >> 1$. Thus, the distance between minima in elastic scattering cross sections measures the nuclear size, while its exponential decay dependence reflects the surface diffuseness.

During the last few years, elastic proton scattering has been one of the major sources of information on the matter distribution of unstable nuclei in radioactive beam facilities. The extended matter distribution of light-halo nuclei (^8He, ^{11}Li, ^{11}Be, etc.) was clearly identified in recent elastic scattering experiments [18,19]. Information on the matter distribution of many nuclei important for the nucleosynthesis in inhomogeneous Big Bang and in r-processes scenarios could also be obtained in elastic scattering experiments. Due to the loosely-bound character and small excitation energies of many of these nuclei, high energy resolution is often necessary. These can be achieved in storage rings by means of electron cooling, or stochastic cooling.

In (p, p') scattering one obtains information on the excited states of the nuclei. For the same reason as in the elastic scattering case, high energy resolutions obtained in storage rings are of crucial relevance [19].

3.2. Transfer Reactions

The cross section for transfer reactions $A(a,b)B$ are given by

$$\frac{d\sigma}{d\Omega} \propto \sum_{lj} S_{AB}(lj)|M_{lj}|^2 \;, \tag{2}$$

where S_{AB} is the spectroscopic factor for the overlap integral of the wave functions of nuclei A and B. If $a = b + x$ (stripping reaction), this integral is given by $\psi_x(\mathbf{r}_{xB}) = \int d\xi \Phi_A^* \, \Phi_B$. In eq. (2), lj denotes the angular momentum quantum numbers of the particle x within B and M_{lj} is an integral of the product of the interaction V_{bx}, the incoming and outgoing scattering states $\chi_a^{(+)}$ ($\chi_x^{(-)}$), and the wave function $R_{njl}(r_{xB})$. Transfer reactions are a well established tool to obtain spin, parities, energy, and spectroscopic factors of states in the $B + x$ system. Experimentally, (d, p) reactions are mostly used due to the simplicity of the deuteron.

The astrophysically relevant nuclear reactions proceed via compound-nucleus reactions (CN) or direct reactions (DR). The decisive mechanism depends on the number of levels in the CN. If there are no resonances in the energy interval relevant for the reaction, one can use the DR models, like direct capture (DC). In this case, $\sigma^{nr} \propto \sum_x S_x \sigma_x^{DC}$, where the sum extends over all bound states in the final nuclei and S_x is the relevant spectroscopic factor. For radiative capture reactions, e.g., $b(x,\gamma)a$, $\sigma_x^{DC} \propto | < \chi_b\chi_x|\mathcal{O}_{\pi\lambda}|\phi > |^2$, where χ are scattering waves, ϕ is the bound-state wave function, and $\mathcal{O}_{\pi\lambda}$ is the electromagnetic operator.

In the case of a single isolated resonance the resonant part of the cross section is given by the Breit-Wigner formula $\sigma_r(E) \propto \Gamma_{in} \Gamma_{out} [(E_r - E)^2 + \Gamma_{tot}^2/4]^{-1}$. The partial widths of the entrance and exit channels are Γ_{in} and Γ_{out}, respectively. The total width Γ_{tot} is the sum over the partial widths of all channels. The particle width Γ_p can be related to the spectroscopic factors S and the single-particle width $\Gamma_{s.p.}$ by $\Gamma_p = C^2 S \Gamma_{s.p.}$, where C is the isospin Clebsch-Gordan coefficient.

If one considers a few resonant states the R-matrix theory is appropriate. In this theory, the resonant part of the cross sections is obtained by a sum of Breit-Wigner functions, slightly displaced (Thomas-Lane correction) in the resonant energy due to the background terms of the other resonances that are superimposed to the considered resonance.

We see that (d, p) reactions are important to astrophysics indirectly to determine the spectroscopic factors for (n, γ). Many of these are unknown and urgently needed for the-

oretical calculations. Examples are the reactions $^7Li(n,\ \gamma)^8Li$ and $^9Be(n,\ \gamma)^{10}Be$ where spectroscopic factors from the $(d,\ p)$ reactions are not known experimentally. Interesting to astrophysics are most $(d,\ p)$ reactions on the neutron rich side of the nuclide card, where no $(d,\ p)$ has been measured before.

If the level density of the CN is so high that there are many overlapping resonances in a certain energy interval the statistical Hauser-Feshbach model can be applied. In an astrophysical plasma one needs to know the transmission coefficients thermally averaged over several populated states

$$T(E, J, \pi) = \sum_{\nu=0}^{\nu_m} T^\nu(E, J, \pi, E_m^\nu, J_m^\nu, \pi_m^\nu) \tag{3}$$
$$+ \int_{E_m^{\nu_m}}^{E-S_m} \sum_{J_m, \pi_m} T(E, J, \pi, E_m, J_m, \pi_m)\, \rho(E_m, J_m, \pi_m)\, dE_m \quad,$$

where S_m is the channel separation energy, and the summation over excited states above the highest experimentally known state ν_m is changed to an integral over the level density ρ. The energy, spin and parities of the states are denoted by E_m, J_m and π_m, respectively.

The necessary condition for application of statistical models is a large number of resonances at the appropriate bombarding energies, so that the cross section can be described by an average over resonances. In the case of neutron–induced reactions a criterion for the applicability can directly be derived from the level density. The relevant energies will lie very close to the neutron separation energy. Thus, one only has to consider the level density at this energy. It is usually said that there should be at least 10 levels per MeV for reliable statistical model calculations. The level densities at the appropriate neutron separation energies are shown in Fig. 4, adapted from ref. [14] (note that therefore the level density is plotted at a *different* energy for each nucleus). One can easily identify the magic neutron numbers by the drop in level density. A general sharp drop is also found for nuclei close to the neutron drip line. For nuclei with such low level densities the statistical model cross sections will become very small and other processes might become important, such as direct reactions [14]. The above plot can give hints on when it is safe to use the statistical model approach.

The use of (d,p) reactions at storage rings has already been proposed for the spectroscopy of neutron resonances in r-processes nuclei close to the magic shells [20]. The two proposed cases (i) $^{46}K(d,\ p)$ and (ii) $^{134}Te(d,\ p)$ are of interest in connection with the interpretation of (i) the $^{48}Ca/^{46}Ca$-abundance anomaly observed in the Allende metereorite [21] and (ii) the $A \sim 130$ r-process abundance peak. For both isotopes a measurement of the spectroscopic factors and spins for transitions to the ground state and the lowest excited states will allow improved calculations of the DR cross section, which is the expected to be the dominant component of the neutron capture rate.

Mass and half-life measurements of neutron deficient isotopes is currently of strong interest. Recently, network calculations have been extended up to the mass 100 (Z=50) and different mass formula have been tested (Hilf, Jaenecke, Möller, etc.) [22]. For the half lives QRPA and partly shell model calculations were used. It turns out that the reaction path and also the time scale for the rapid proton capture process are strongly determined by the masses. This is in particular very important in the mass-80 region

where large deformation effects have to be considered. Also to be measured needs to be the decay of the isotopes along the N=Z line in this mass range. The measurement of ^{80}Zr has just been completed and of ^{84}Mo has been proposed [22]. But, there is still a lot more to be done.

3.3. Trojan Horse

In order for transfer reactions $A(a, b)B$ to be effective, a matching condition between the transferred particle and the internal particle momenta has to exist. Thus, beam energies should be in the range of a few 10 MeV per nucleon. It has been proposed that low energy reactions of astrophysical interest can be extracted directly from breakup reactions $A + a \longrightarrow b + c + B$ by means of the Trojan Horse effect [23]. If the Fermi momentum of the particle x inside $a = (b + x)$ compensates for the initial projectile velocity v_a, the low energy reaction $A + x = B + c$ is induced at very low (even vanishing) relative energy between A and x. To show this, one writes the DWBA cross section for the breakup reaction as $d^3/d\Omega_b d\Omega_c dE_b \propto |\sum_{lm} T_{lm}(\mathbf{k_a}, \mathbf{k_b}, \mathbf{k_c}) S_{lx} Y_{lm}(\mathbf{k_c})|^2$, where $T_{lm} = <\chi_b^{(-)} Y_{lm} f_l | V_{bx} | \chi_a^+ \phi_{bx}>$. The threshold behaviour E_x for the breakup cross section $\sigma_{A+x \to B+c} = (\pi/k_x^2) \sum_l (2l + 1) |S_{lx}|^2$ is well known: since $|S_{lx}| \sim \exp(-2\pi\eta)$, then $\sigma_{A+x \to B+c} \sim (1/k_x^2) \exp(-2\pi\eta)$. In addition to the threshold behaviour of S_{lx}, the breakup cross section is also governed by the threshold behaviour of $f_l(r)$, which for $r \longrightarrow \infty$ is given by $f_{l_x} \sim (k_x r)^{1/2} \exp(\pi\eta) K_{2l+1}(\xi)$, where K_l denotes the Bessel function of the second kind of imaginary argument. The quantity ξ is independent of k_x and is given by $\xi = (8r/a_B)^{1/2}$, where $a_B = \hbar^2/m Z_A Z_x e^2$ is the Bohr length. From this one obtains that $d^3/d\Omega_b d\Omega_c dE_b \xrightarrow[E_x \to 0]{}$ const.. The coincidence cross section tends to a constant which will in general be different from zero. This is in striking contrast to the threshold behavior of the two particle reaction $A + x = B + c$. The strong barrier penetration effect on the charged particle reaction cross section is canceled completely by the behaviour of the factor T_{lm} for $\eta \to \infty$. Thus, from a measurement of the breakup reaction $A + a \longrightarrow b + c + B$ and a theoretical calculation of the factors T_{lm} one could extract the S-matrix elements S_{lx} needed for the reaction $A + x = B + c$. Basically, this technique extends the method of transfer reactions to continuum states.

Among candidates to be studied with this method at storage rings, one might consider to investigate the reaction $^{18}O(p, \alpha)^{15}N$ by means of the reaction $^{18}O + (b+p) \longrightarrow b + \alpha + ^{15}N$ where $a = (b+p) = d$, ^3He, α, ... The same could be applied to the reactions $^{15}N(p, \alpha)$ or $^{17}O(p, \alpha)$, relevant for the CNO cycle. Also, the reaction $\alpha + ^3He \to ^7Be + \gamma$, which is relevant for the solar neutrino problem, could be investigated e.g. in the reaction $^{16}O + ^3He \to^{12}C + \gamma +^7Be$.

3.4. Asymptotic Normalization Coefficients

The amplitude for the radiative capture cross section $b + x \longrightarrow a + \gamma$ is given by $M = < I_{bx}^a(\mathbf{r_{bx}}) | \mathcal{O}(\mathbf{r_{bx}}) | \psi_i^{(+)}(\mathbf{r_{bx}}) >$, where $I_{bx}^a = < \phi_a(\xi_b, \xi_x, \mathbf{r_{bx}}) | \phi_x(\xi_x) \phi_b(\xi_b) >$ is the integration over the internal coordinates ξ_b, and ξ_x, of b and x, respectively. For low energies, the overlap integral I_{bx}^a is dominated by contributions from large r_{bx}. Thus, what matters for the calculation of the matrix element M is the asymptotic value of $I_{bx}^a \sim C_{bx}^a W_{-\eta_a, 1/2}(2\kappa_{bx} r_{bx})/r_{bx}$, where C_{bx}^a is the asymptotic normalization coefficient (ANC) and W is the Whittaker function. This coefficient is the product of the spectroscopic

factor and a normalization constant which depends on the details of the wave function in the interior part of the potential. Thus, C_{bx}^a is the only unknown factor needed to calculate the direct capture cross section. These normalization coefficients can be found from: 1) analysis of classical nuclear reactions such as elastic scattering [by extrapolation of the experimental scattering phase shifts to the bound state pole in the energy plane], or 2) peripheral transfer reactions whose amplitudes contain the same overlap function as the amplitude of the corresponding astrophysical radiative capture cross section [24].

To illustrate this technique, let us consider the proton transfer reaction $A(a, b)B$, where $a = b + p$, $B = A + p$. Using the asymptotic form of the overlap integral the DWBA cross section is given by $d\sigma/d\Omega = \sum_{J_B j_a} [(C_{Ap}^a)^2/\beta_{Ap}^2][(C_{bp}^a)^2/\beta_{bp}^2]\tilde{\sigma}$ where $\tilde{\sigma}$ is the reduced cross section not depending on the nuclear structure, β_{bp} (β_{Ap}) are the asymptotic normalization of the shell model bound state proton wave functions in nucleus $a(B)$ which are related to the corresponding ANC's of the overlap function as $(C_{bp}^a)^2 = S_{bp}^a \beta_{bp}^2$. Here S_{bp}^a is the spectroscopic factor. Suppose the reaction $A(a, b)B$ is peripheral. Then each of the bound state wave functions entering $\tilde{\sigma}$ can be approximated by its asymptotic form and $\tilde{\sigma} \propto \beta_{Ap}^2 \beta_{bp}^2$. Hence $d\sigma/d\Omega = \sum_{j_i} (C_{Ap}^a)^2(C_{bp}^a)^2 R_{Ba}$ where $R_{Ba} = \tilde{\sigma}/\beta_{Ap}^2 \beta_{bp}^2$ is independent of β_{Ap}^2 and β_{bp}^2. Thus for surface reactions the DWBA cross section is actually parameterized in terms of the product of the square of the ANC's of the initial and the final nuclei $(C_{Ap}^a)^2(C_{bp}^a)^2$ rather than spectroscopic factors. This effectively removes the sensitivity in the extracted parameters to the internal structure of the nucleus.

Recently, this technique has been applied to the reaction $^7Be(d, n)$ at $E_{c.m.} = 5.8$ MeV to determine the asymptotic normalization for ^8B [25]. The astrophysical $S_{17}(0)$ factor for the $^7Be(p, \gamma)^8B$ reaction was derived to be 27.4 ± 4.4 eV.b through the asymptotic normalization coefficient extracted from the experimental data. This is a rather high value, compared to previous measurements, as can be seen from figure 3.

3.5. Charge-exchange, *(p,n)*, Reactions

Charge exchange induced in (p, n) reactions are often used to obtain values of Gamow-Teller matrix elements which cannot be extracted from beta-decay experiments. This approach relies on the similarity in spin-isospin space of charge-exchange reactions and β-decay operators. As a result of this similarity, the cross section $\sigma(p, n)$ at small momentum transfer q is closely proportional to $B(GT)$ for strong transitions [26].

The efficiency of many ν detectors (^{37}Cl, the proposed ^{115}I and ^{127}I detectors, etc.) depends on the cross section for absorption of neutrinos, through inverse β decay, in the detector material. When corresponding matrix elements for allowed GT beta decay cannot be measured in β decay experiments, for example, if the β decay is not energetically allowed, it is common to obtain these matrix elements using charge exchange reactions.

Such experiments could be carried out using storage rings. However, there is some debate if the accuracy of (p, n) reactions as a calibration of solar neutrino detectors can be achieved. As shown in ref. [27], for important GT transitions whose strength are a small fraction of the sum rule the direct relationship between $\sigma(p, n)$ and $B(GT)$ values fails to exist. Similar discrepancies have been observed [28] for reactions on some odd-A nuclei including ^{13}C, ^{15}N, ^{35}Cl, and ^{39}K and for charge-exchange induced by heavy ions [29].

3.6. Coulomb Dissociation Method

We now consider projectile breakup reactions $a + A \longrightarrow b + x + A$ in which (a) the target A remains in the ground state, (b) the nuclear contribution to the breakup is small, and (c) the breakup is a first order process. Then the (differential, or angle integrated) breakup cross section can be written as $\sigma_C^{\pi\lambda}(\omega) = F^{\pi\lambda}(\omega) \cdot \sigma_\gamma^{\pi\lambda}(\omega)$, where ω is the energy transferred from the relative motion to the breakup, and $\sigma_\gamma^{\pi\lambda}(\omega)$ is the photo nuclear cross section for the multipolarity $\pi\lambda$ and photon energy ω. The function $F^{\pi\lambda}$ depends on ω, the relative motion energy, and nuclear charges and radii. They can be very accurately calculated [30] for each multipolarity $\pi\lambda$.

Time reversal allows one to deduce the radiative capture cross section $b + x \longrightarrow a + \gamma$ from $\sigma_\gamma^{\pi\lambda}(\omega)$. Thus, assuming that the conditions (a–c) apply, the Coulomb dissociation can be used to deduce $\sigma(b + x \longrightarrow a + \gamma)$. This method was proposed in ref. [31]. It has been tested successfully in a number of reactions of interest for astrophysics. For example, the $d(\alpha, \gamma)^6Li$, relevant for the evolution of the primordial fireball has been measured down to 100 keV by using the breakup of 156 MeV ^6Li ions on several targets [32]. They have obtained the only 5 points in the energy interval 100–710 keV, previously unaccessible by direct capture experiments. Another case was the $^{13}N(p, \gamma)^{14}O$ reaction which was studied via the $^{14}O \longrightarrow^{13} N + p$ Coulomb dissociation on heavy targets [33]. The $^{13}N(p, \gamma)^{14}O$ reaction is very important for the CNO cycle when its rate becomes faster than $^{13}N\beta$-decay. This leads to a breakout of the CNO-cycle. The rate of this reaction is essentially determined by the gamma width Γ_γ of the 5.173 MeV 1^- resonance of ^{14}O. The value obtained with the Coulomb dissociation method (CDM) $\Gamma_\gamma = (3.1\pm0.6)$ eV, compares well with the result from direct capture experiments. For a review of the results obtained with the CDM, see ref. [34] and references therein. Worth quoting is the recent experiment where the reaction $^7Be(p,\gamma)^8B$ has been studied with the CDM [35]. They have obtained an $S_{17}(0)$ value of 16.7 eV.b which is about 20% smaller than the value commonly used in solar model calculations [9]. However, this CDM experiment yields a rather large $E2$ breakup cross section which has to be subtracted from the total breakup cross section in order to allow the determination of the E1 radiative capture cross, which dominates at low $^7Be - p$ energies. Work in this direction is under way in several laboratories. For this reaction, the dominance of the Coulomb interaction in the dissociation process, and the validity of first-order perturbation theory have been demonstrated theoretically [36].

In storage rings a series of reactions could be studied using the CDM, depending on the luminosities: (a) $^4He(d,\gamma)^6Li$, $^6Li(p,\gamma)^7Be$, $^6Li(\alpha, \gamma)^{10}B$, $^4He(t,\gamma)^7Li$, $^7Li(\alpha, \gamma)^{11}B$, $^{11}B(p, \gamma)^{12}C$, $^9Be(p, \gamma)^{10}B$, and $^{10}B(p, \gamma)^{11}C$, [primordial nucleosynthesis of Li, Be, and B-isotopes], (b) $^{12}C(n, \gamma)^{13}C$, $^{14}C(n, \gamma)^{15}C$, and $^{14}C(\alpha, \gamma)^{18}O$ [inhomogeneous Big Bang nucleosynthesis], (c) $^{12}C(p, \gamma)^{13}N$, $^{16}O(p, \gamma)^{17}F$, $^{13}N(p,\gamma)^{14}O$, and $^{20}Ne(p, \gamma)^{21}Na$ [CNO-cycle], (d) $^{31}S(p, \gamma)^{32}Cl$ [rapid proton capture process], and (e) $^{12}C(\alpha, \gamma)^{16}O$, $^{16}O(\alpha, \gamma)^{20}Ne$, and $^{14}N(\alpha, \gamma)^{18}F$ [helium burning]. The projectiles are either stable, or have a half-life larger than a few seconds. Of course, one of the most interesting cases is the reaction $^{12}C(\alpha, \gamma)^{16}O$, or the triple-alpha capture reaction $3\alpha \longrightarrow^{12} C$, both relevant for the fate of massive stars. However, due to the large energy ($\sim$ 7 MeV) required to disrupt ^{12}C, or ^{16}O, the nuclear contribution to the breakup process is large. Nonetheless, Coulomb dissociation might be an alternative if special kinematical conditions are chosen.

REFERENCES

1. E.E. Salpeter, Aust. J. Phys. 7 (1954) 373.
2. H.J. Assenbaum, K. Langanke and C. Rolfs, Z. Phys. A327 (1987) 461.
3. S. Engstler *et al.*, Phys. Lett. B202 (1988) 179.
4. G. Blügge and K. Langanke, Phys. Rev. C41 (1990) 1191; K. Langanke and D. Lukas, Ann. Phys. 1 (1992) 332.
5. C. Rolfs and E. Somorjai, Nucl. Inst. Meth. B99 (1995) 297.
6. T. Kajino, Nucl. Phys. A588 (1995) 339c.
7. T. Paradellis *et al.*, Z. Phys. A337 (1990) 211.
8. R.N. Boyd *et al.*, Phys. Rev. Lett. 68 (1992) 1283.
9. J.N. Bahcall, "Neutrino Astrophysics", Cambridge University Press, 1989.
10. F.C. Barker, Aust. J. Phys. **33** (1980) 177; Phys. Rev. **C37** (1988) 2930.
11. F. Hoyle, D.N. Dunbar, W.A. Wenzel and W. Whaling, Phys. Rev. 92 (1953) 1095.
12. S.E. Woosley, Proceedings of the Accelerated Radioactive Beam Workshop, eds. Buchmann and J.M. D'Auria (TRIUMF, Canada, 1985).
13. L. Buchmann *et al.*, Phys. Rev. Lett. 70 (1993) 726; Z. Zhao *et al.*, Phys. Rev. Lett. 70 (1993) 2066.
14. H. Oberhummer, H. Herndl, T. Rauscher and H. Beer, University of Vienna, preprint 1996, to be published.
15. M. Jung *et al.*, Phys. Rev. Lett. 69 (1992) 2164.
16. F. Bosch *et al.*, GSI/Darmstadt Scientific Report, 1995.
17. F. Bosch, Spokesperson, GSI/Darmstadt experiment proposal E019, 1996.
18. S. Neumaier *et al.*, Nucl. Phys. A583 (1995) 799.
19. A.A. Korsheninnikov *et al.*, Proceedings of the Int. Workshop on Physics of Unstable Nuclear Beams, (Serra Negra, Brazil, 1996), eds. C.A. Bertulani, L.F Canto and M.S. Hussein, World Scientific, in press.
20. P. Egelhof and K.L. Kratz, spokepersons, GSI/Darmstadt proposal E023.
21. D.G. Sandler, S.E. Koonin and W.F. Fowler, Ap. J. 259 (1982) 908.
22. M. Wiescher, private communication.
23. G. Baur, Phys. Let. B178 (1986) 135.
24. A.M. Mukhamedzhanov and N.K. Timofeyuk, JETP Lett. 51 (1990) 282.
25. Weiping Liu *et al.*, Phys. Rev. Let. 77 (1996) 611.
26. T.N. Tadeucci *et al.*, Nucl. Phys. A469 (1987) 125.
27. S.M. Austin, N. Anantaraman and W.G. Love, Phys. Rev. Lett. 73 (1994) 30.
28. J.W. Watson et al., Phys. Rev. Lett. 55 (1985) 1369.
29. C.A. Bertulani and P. Lotti, to be published.
30. C. Bertulani and G. Baur, Phys. Reports 163 (1988) 299.
31. G. Baur, C. Bertulani and H. Rebel, Nucl. Phys. A459 (1986) 188.
32. J. Kiener et al., Phys. Rev. C44 (1991) 2195.
33. T. Motobayashi et al., Phys. Lett. B264 (1991) 259.
34. G. Baur and H. Rebel, J. Phys. G20 (1994) 1.
35. T. Motobayashi et al., Phys. Rev. Lett. 73 (1994) 2680.
36. C. Bertulani, Nucl. Phys. A587 (1995) 318; Phys. Rev. C49 (1994) 2688; Z. Phys. A, to be published.